



Han, D., Yang, K. and Barakos, G. N. (2018) Extendable chord for improved helicopter rotor performance. *Aerospace Science and Technology*, 80, pp. 445-451. (doi:[10.1016/j.ast.2018.07.031](https://doi.org/10.1016/j.ast.2018.07.031))

This is the author's final accepted version.

There may be differences between this version and the published version. You are advised to consult the publisher's version if you wish to cite from it.

<http://eprints.gla.ac.uk/165586/>

Deposited on: 19 July 2018

Enlighten – Research publications by members of the University of Glasgow

<http://eprints.gla.ac.uk>

# Extendable Chord for Improved Helicopter Rotor Performance

Dong Han

National Key Laboratory of Science and Technology on Rotorcraft Aeromechanics, College of Aerospace Engineering,  
Nanjing University of Aeronautics and Astronautics, Nanjing 210016, China

Email: [donghan@nuaa.edu.cn](mailto:donghan@nuaa.edu.cn)

Kelong Yang

National Key Laboratory of Science and Technology on Rotorcraft Aeromechanics, College of Aerospace Engineering,  
Nanjing University of Aeronautics and Astronautics, Nanjing 210016, China

Email: [yangkelong@nuaa.edu.cn](mailto:yangkelong@nuaa.edu.cn)

George N. Barakos

CFD Laboratory School of Engineering, University of Glasgow, G12 8QQ, Scotland, UK

Email: [George.Barakos@glasgow.ac.uk](mailto:George.Barakos@glasgow.ac.uk)

Extendable blade sections are investigated as a method for reducing rotor power and improving helicopter performance. A validated helicopter power prediction method, based on an elastic beam model is utilized. The static extendable chord can deliver a rather small power reduction in hover, and significant power savings at high speed flight, however, the cruise power is increased. In hover, the active chord is best deployed in the middle part of the blade, and just inboard of the tip at high speed flight. The increase in chord length can lead to power savings at high speed flight but the benefits decrease in other speeds. The 1/rev dynamically extendable chord can lead to an overall power reduction over the speed range of a helicopter. The best deployment location is at the blade tip, which is different from the statically extendable chord. It is best extended out in the retreating side, and retracted back in the advancing. The power reduction by the 1/rev dynamically extendable chord increases with the increase in the length of the chord extension and take-off weight of the helicopter. Generally, a lower harmonic extendable chord can save more power than one actuated at higher harmonics. The dynamic chord can reduce more power than the corresponding static chord.

Keywords: extendable chord; helicopter; rotor; performance; static extension; dynamic extension

## 1. Introduction

Rectangular rotor blades are convenient for manufacturing, but not optimal for aerodynamic performance, so rotor blade plan-form optimization is an effective method to reduce rotor power in hover and forward flight, and improve helicopter performance. In 1940s, blade taper was investigated to improve hover performance, and a taper ratio of 3 to 1 could increase the rotor thrust by approximately 2 to 3 percent [1]. Effort has also been put to optimize the blade plan-form, but most helicopter rotors still adopt rectangular blades. The use of composites makes practical to fabricate non-rectangular rotor blades, especially with advanced blade tips. Passive rotor blade shape design has seen great progress leading to improvements of helicopter rotor performance [2-4], and the aerodynamic parameters could be optimized to balance the requirement and obtain more performance improvement [5-8]. To further improve rotor performance is, however, a challenging topic.

Léon et al. examined quasi-statically extendable chord sections to improve helicopter performance near the envelope boundaries [9]. The analyses based on the UH-60 helicopter showed an expansion of the flight envelope.

Khoshlahjeh and Gandhi investigated extendable chord rotors for flight envelope expansion and performance improvement [10]. The analyses were based on the quasi-steady trailing-edge plate and showed significant power reduction at high gross weight and altitude, and performance improvement at maximum speed, gross weight and altitude. The trailing-edge plate reduced the angle of attack in the retreating side, and shifted the lift inboard. This offloading of the blade tips reduced the drag and torque, and the rotor power was consequently reduced. Among active blade controls, the extendable blade chord has shown significant potential in reducing rotor power, especially at high speed flight [11]. The 1/rev dynamic blade chord reduces the blade chord length in the advancing side to alleviate compressibility effects, and increases it in the retreating side to lower the angle of attack of the blade and delay stall. This way, the rotor profile drag can be reduced and rotor power can be saved. Past research concentrated on the effect of the static or 1/rev extendable chord on the performance improvement of helicopters, especially near the flight envelope boundary. Nevertheless, the question whether static or dynamic chord extension is better for rotor performance should be addressed. The same is true for the identification of the optimal location of the extendable chord and the best harmonic excitation.

This work focuses on the potential of static and dynamic chords in reducing helicopter rotor power. The dynamic chord is not limited to 1/rev, and higher harmonics are also investigated. Parametric analyses are conducted to enhance the potential of chord extension in the flight performance improvement of helicopters.

## 2. Modeling and Validation

### 2.1 Performance Prediction Method

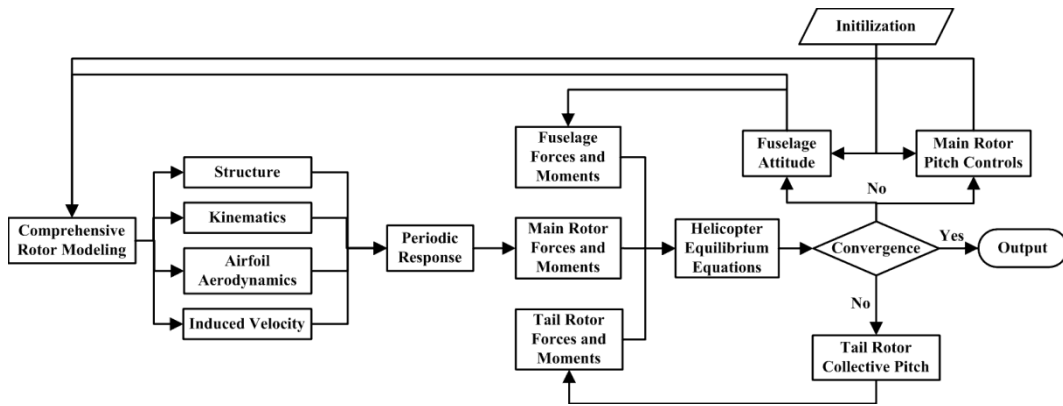


Figure 1: Flowchart of performance prediction.

A helicopter model is utilized, which includes a rotor model, a tail rotor model, a fuselage model and a propulsive trim method. The rotor model is based on an elastic beam model with moderate deflections, which can capture the geometric nonlinearity of advanced helicopter blades. The blade rotations about the blade hinges and rotor shaft are introduced as generalized coordinates. Look-up aerofoil aerodynamics is used. The induced velocity over the rotor disk is captured by the Pitt-Peters inflow model [12]. The equations of motion of the system are derived based on the generalized force formulation. The Newmark integration method is utilized to calculate the steady response of the rotor in the time domain [13]. The hub forces and moments of the main rotor are derived from the resultant root forces and moments of the blades. The fuselage is treated as a rigid body with aerodynamic forces and moments. The thrust and power of the tail rotor are determined by momentum theory with the uniform inflow model.

Given the initial values of the pitch controls and the fuselage attitude angles, the steady response of the rotor can be

obtained at a prescribed forward speed, flight altitude and take-off weight. The hub forces and moments of the main rotor are balanced by the forces and moments acting on the fuselage and tail rotor. These component forces and moments constitute the equilibrium equations of the helicopter, which are solved to update the pitch controls and attitude angles. After some iterative computation of the periodic response of the rotor and solutions of the equilibrium equations, the trimmed pitch controls and attitude angles can be obtained. Then the main rotor power and related information of the helicopter can be derived. The flowchart is shown in Figure 1. This modeling methodology has been used to analyze the transient aeroelastic responses of shipboard rotors and the helicopter performance improvement by variable rotor speed and variable blade twist [14, 15].

## 2.2 Validation

The flight data of the UH-60A helicopter is utilized to validate the methodology used in this work [16]. The parameters of the main rotor and tail rotor are provided in Ref. 17. The distributions of the airfoil and blade pre-twist of the main rotor are given in Ref. 18. For performance analysis, a model of the aerodynamic fuselage drag can provide acceptable predictions [16]. The fuselage drag equation utilized in the present work is

$$\frac{D}{q} \text{ (ft}^2\text{)} = 35.83 + 0.016 \times (1.66\alpha_s^2) \quad (1)$$

where,  $D$  is the fuselage drag,  $q$  is the dynamic pressure, and  $\alpha_s$  is the aircraft pitch angle. In this work, the geometric parameters of the baseline helicopter are the same as the UH-60A helicopter. To reduce the effect of the flexibility of the blade structure on the rotor performance, a hingeless rotor blade with uniform blade properties is utilized. The fundamental flap, lag and torsional frequency ratios of the baseline rotor at full rotor speed are taken as 1.14, 1.40 and 6.50, respectively. The comparisons of the prediction of rotor power with the flight test data for the take-off weight coefficients 0.0065, 0.0074, 0.0083 and 0.0091, are shown in Figure 2. It is obvious that the predictions by the present method are generally in good agreement with the flight test data for these take-off weights, which verifies the use of the present method in analyzing helicopter performance.

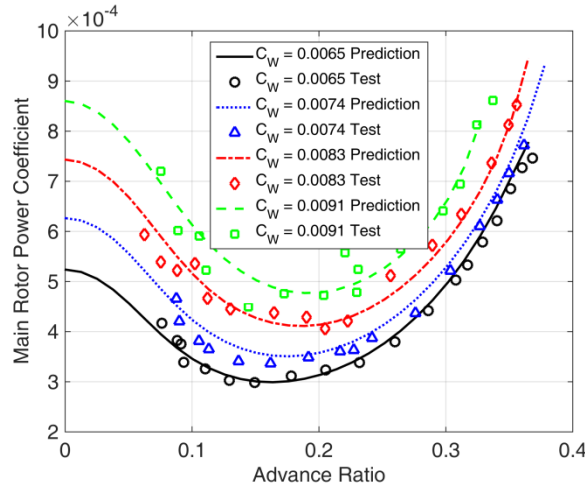


Figure 2: Comparison of the prediction with the flight data.

## 2.3 Airfoil Aerodynamics

An extendable chord can change the chord length and modify the aerodynamic characteristics of the airfoil. Given a

suitable deployment angle ( $\delta=2^\circ$ ) of the extendable chord [10], as shown in Figure 3, there is virtually no change in the aerodynamic lift coefficient. Since this work focuses on the effect of the static and dynamic chord extension on rotor performance, the study of the effect of the extendable chord on the airfoil aerodynamics is omitted from this paper. The lift, drag and moment coefficients  $\bar{C}_l$ ,  $\bar{C}_d$  and  $\bar{C}_m$  for an airfoil with an extendable chord are related with the baseline coefficients  $C_l$ ,  $C_d$  and  $C_m$  as [10]

$$\begin{cases} \bar{C}_l = (1 + \varepsilon)C_l \\ \bar{C}_d = (1 + \varepsilon)C_d \\ \bar{C}_m = (1 + \varepsilon)^2C_m \end{cases} \quad (2)$$

where,  $\varepsilon$  represents the chord extension as a percentage of the baseline chord length  $c$ . The effect of the chord extension is equivalent to an increase in the aerodynamic coefficients.

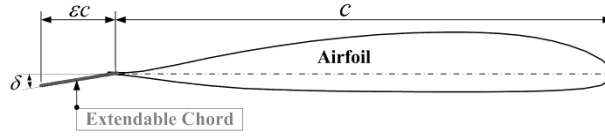


Figure 3: Configuration of extendable Chord.

### 3. Performance Improvement

The following analysis is based on the UH-60 helicopter, and the baseline flight state is at sea level and a take-off weight of 9474.7kg (weight coefficient 0.0074). In the following analyses, the four extendable chords with 10%R (R, rotor radius) as the width (Location 1, 2, 3 and 4) are investigated, as shown in Figure 4. The start points of the locations are 52.3%R, 62.3%R, 72.3%R and 85.4%R. The configurations of statically or dynamically extendable chords are explored to improve rotor performance in hover and forward flight. For the statically extendable chord, the corresponding chord length does not change with the azimuth. For the dynamically extendable chord, the length varies by a prescribed harmonic motion.

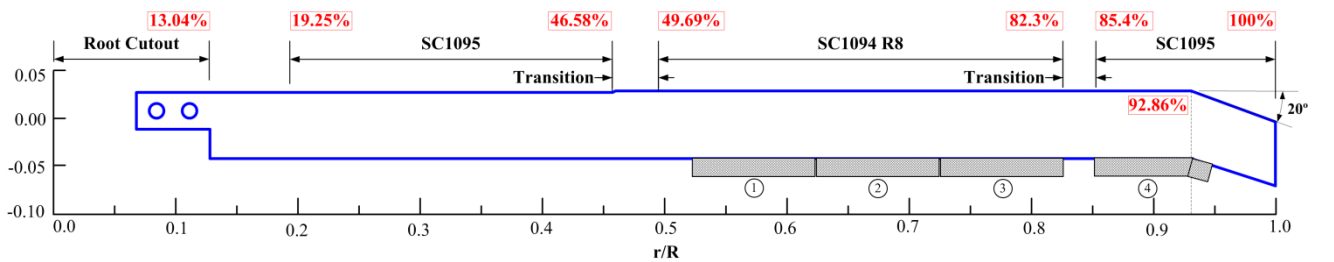


Figure 4: The configuration of an extendable chord vs. the UH-60A[19] rotor as baseline.

The power reduction ratio is defined to determine the benefits in rotor power savings as

$$\eta = (1 - P/P_b) \times 100\% \quad (3)$$

where,  $P$  is the rotor power with the extendable chord and  $P_b$  is the baseline rotor power without any extendable chord.

#### 3.1 Statically Extendable Chord (SEC)

The extendable chord length is set to be 20% of the blade chord i.e.  $\varepsilon=20\%$ . Figure 5 explores the location of the SEC on the rotor power reduction. In hover, the required rotor power increases as the extendable chord approaches the blade tip. The SEC is best placed in the middle part of the blade (Location1). In addition, the power reduction at Location 1 is rather small. At cruise, the power reduction is negative, which means some extra power is needed for the rotor with the SEC. At high speed flight, the benefit in power saving emerges. At a speed of 300km/h, the power reductions are 0.37%, 0.96%, 1.27% and 0.55% at Locations 1, 2, 3 and 4, respectively. The SEC can be used to reduce rotor power and improve helicopter performance at high speed flight. The power saving at the Location 3 is better than at Location 4, which indicates that the best location for the power reduction at high speed flight is not the tip but inboard of it. At a speed of 300km/h, the chord extension from 62.3%R to 82.3%R (Location 2+3 shown in Figure 5) can reduce the power by 1.90%, which is more than the value at Locations 2 or 3. A larger chord extension is preferred at high speed flight. The power reduction of 1.90% is less than the sum of 0.96% and 1.27%, which indicates that the power reduction is not a linear addition of the benefit at the two sections.

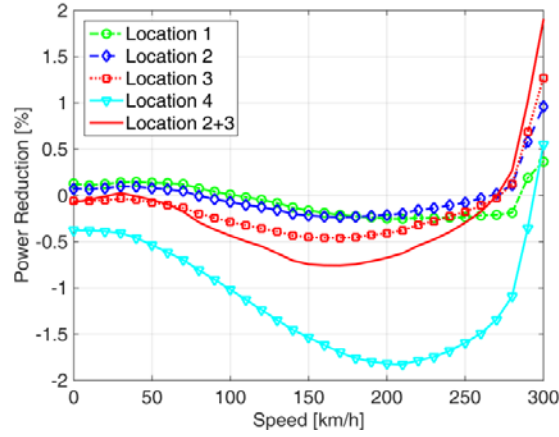
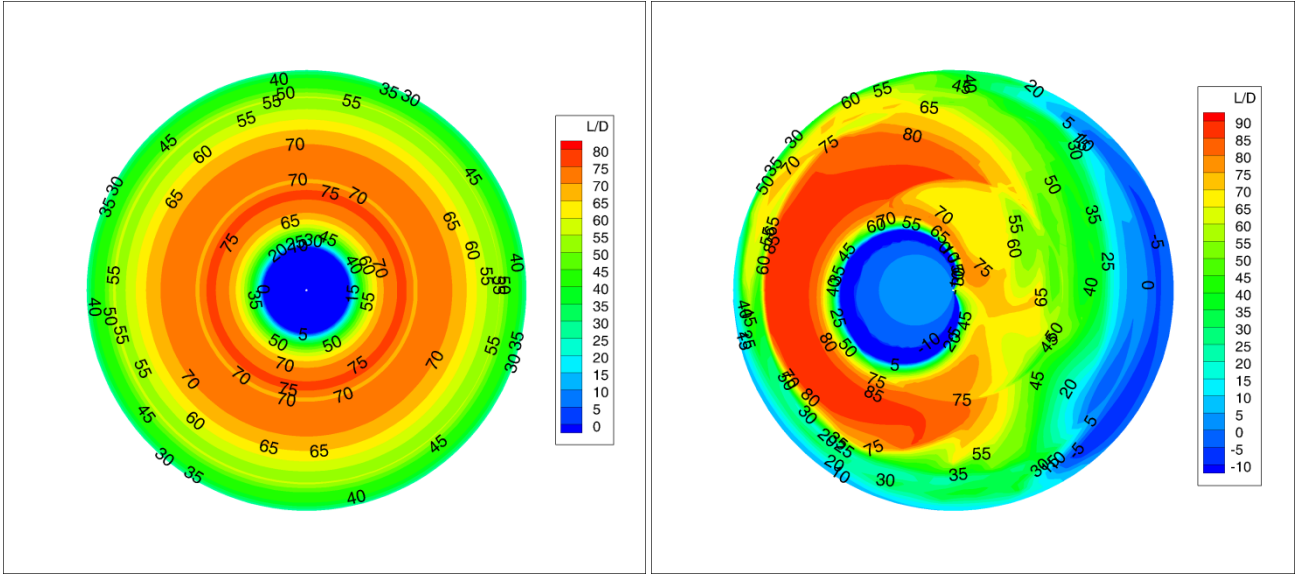


Figure 5: Power reduction for different location of the chord.

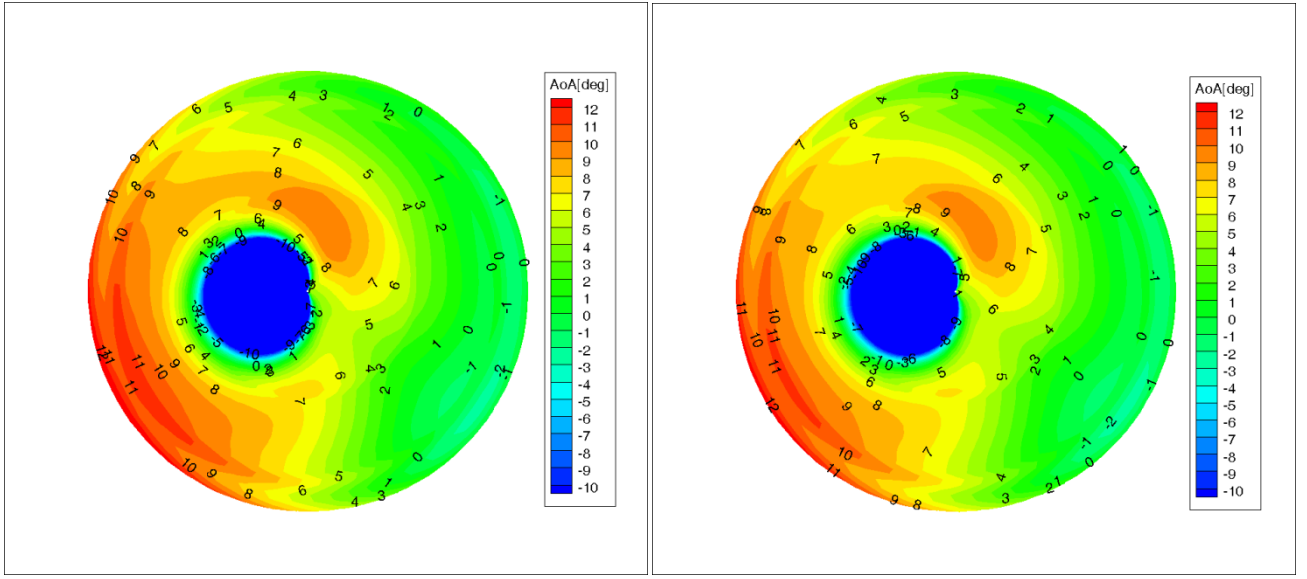


(a) hover

(b) 300km/h

Figure 6: Distribution of L/D over the rotor disk.

Different deployment locations of the SEC have different effects on the rotor power at different flight speeds. Figure 6 shows the distribution of lift to drag ratio ( $L/D$ ) of airfoil sections over the rotor disk in hover and 300km/h forward speed without any SEC. In hover, the largest value of  $L/D$  is located at about 35%R-75%R. In the inner or outer part of the blade, the efficiency becomes lower, and it is obvious that these locations are not suitable for the deployment of the SEC. At high speed flight, the most efficient part of the blade that generates lift in the advancing side, moves inboard and the corresponding part in the retreating side moves outboard. The SEC is best placed inboard and close to the blade tip region to balance the efficiency in the advancing and retreating sides. The longest chord of the high speed helicopter X2 locating at around 75%R affirms this point [20].



(a) baseline

(b) with SEC (Location 3)

Figure 7: Distribution of AoA over the rotor disk.

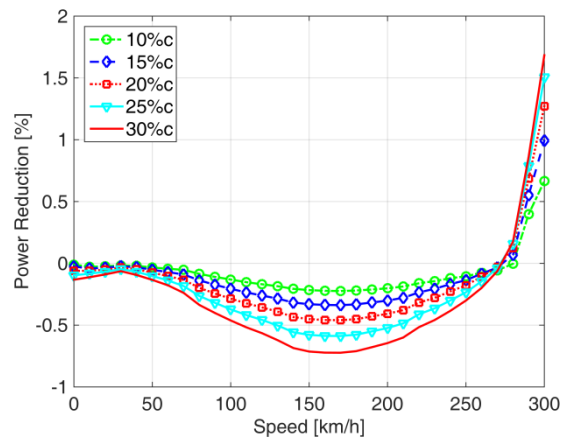


Figure 8: Power reduction for different chord length of SEC.

Figure 7 shows the distribution of the angle of attack (AoA) over the rotor disk with and without the SEC at a speed of 300km/h. The AoA on the retreating side decreases significantly, especially near the area of  $8^\circ$ . The increase in the

chord length increases the rotor solidity, and more blade area can be used to generate lift. Naturally it lowers the AoA and delays the stall in the retreating side. In the analysis, the rotor solidity increases by 2%. This value is rather small, and naturally the value of power reduction is small.

Figure 8 shows the effect of the extendable chord length of the SEC on the power reduction (Location 3). From hover to medium high speed flight, the power can't be reduced. At high speed flight, the power reduction increases sharply. In hover and low speed flight, the effect of the length is substantially small, and the power increase by the SEC is limited. At cruise, the power increase is significant, and it is not beneficial to deploy the SEC. At high speed flight, a larger chord length is preferred. Results show that 30% chord extension, which corresponds to an increase in solidity of 3%, reduces the power by 1.68%. From the point of view of power saving, the SEC is more suitable to be deployed at high speed flight.

### 3.2 Dynamically Extendable Chord (DEC) with 1/rev Input

For the DEC, the chord length is prescribed as

$$\varepsilon = A[1.0 + \sin(n\Omega t + \phi)] \quad (4)$$

where,  $A$  is the amplitude of input,  $n$  is the harmonic number,  $\Omega$  is the rotor speed, and  $\phi$  is the phase of the input.

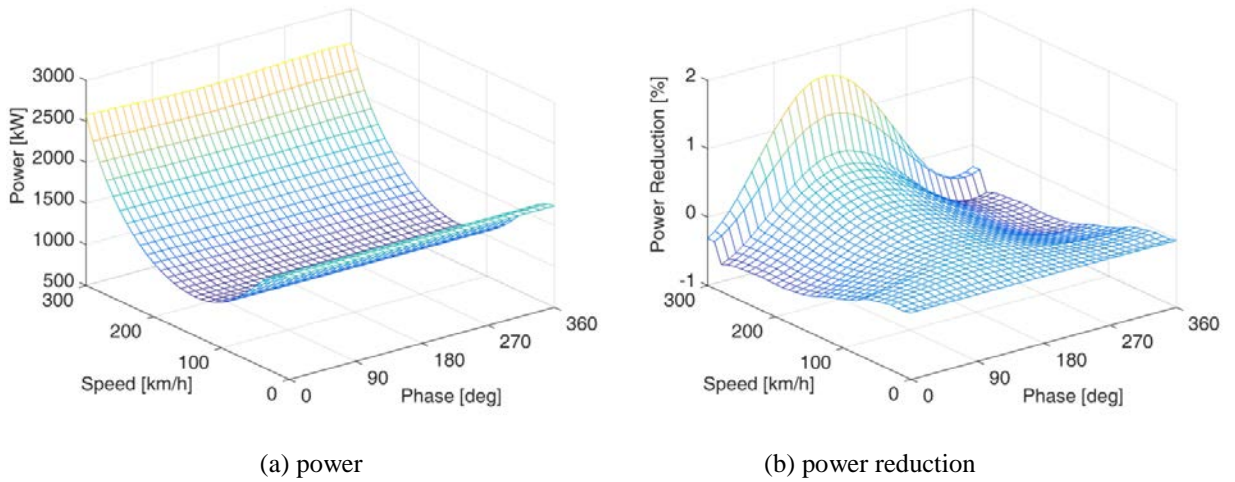


Figure 9: Power and power reduction for the 1/rev input.

In the following analysis, the DEC is placed at Location 3 with an amplitude of 10%c. Figure 9 presents the effect of the phase of 1/rev input on the rotor power and power reduction. In hover and low speed forward flight, the change of the power is rather limited. With the increase in the forward speed, the power reduction can be increased when the phase shifts to a suitable angle. At a speed of 300km/h, the power reduction can be maximized to be 1.60%. This value is 1.26 times the value obtained by the SEC with the 20%c extension. In terms of power saving, the concept of DEC is better than the SEC. Another benefit is that it can lead to an overall power reduction over the speed range, and almost zero power reduction in hover, and very low speed flight. The phase corresponding to the maximum power reduction is 160°, and it does not change with the speed. At this phase, the chord retracts back in the blade in the advancing side, and extends out in the retreating side. It is obvious that the extension of the chord could reduce the AoA in the retreating side and delay the stall. The retraction in the advancing side can reduce the drag compared with the SEC. The SEC cannot deliver this and results in lower power reduction. Figure 10 shows the distribution of the AoA over the rotor disk with the



DEC at a speed of 300km/h. The primary change is the decrease of the AoA in the retreating side compared with the baseline distribution shown in Figure 7. It leads to the delay of the blade stall and power savings. This distribution is similar as the SEC.

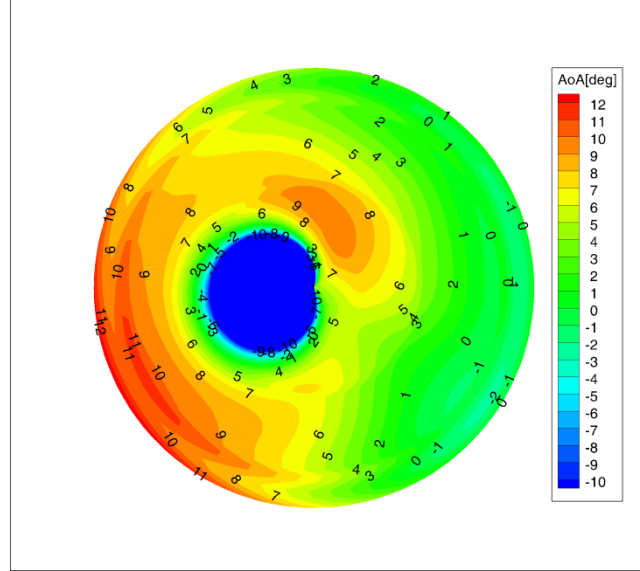


Figure 10: The distribution of AoA over the rotor disk with DEC.

Figure 11 shows the effect of the amplitude of the input on the power reduction at different flight speeds. It is evident that the power reduction increases with the amplitude. The increase is almost linear, with a small decrease of rate at larger extensions. The power can be reduced in low to medium high speed, but the benefits are rather small. This confirms that the deployment of DEC is more suitable at high speed flight. Increasing the extendable length is effective in improving the performance of DEC.

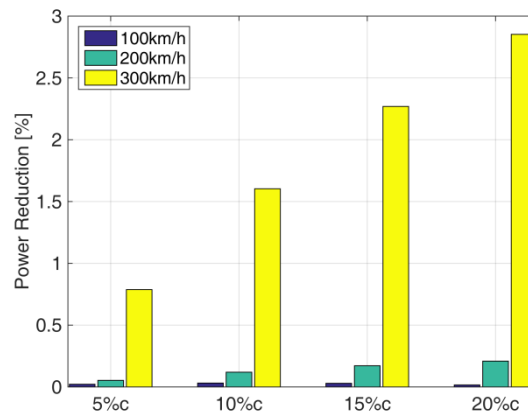


Figure 11: The effect of input amplitude on the power reduction.

Figure 12 shows the effect of the location of the DEC on the power reduction. It is obvious that the best location is the blade tip (Location 4), which is different from that of the SEC (Location 3). Compared with the power reduction at Location 3 and the phase of  $160^\circ$ , the power reduction at Location 4 increases by 40%. This is a significant improvement,

showing that DEC is best placed at the blade tip. For different locations, the optimum phase of the DEC is almost the same. At Location 1, the phase is  $180^\circ$ , and it shifts to  $160^\circ$  at Location 4, indicating that the DEC is best deployed on the retreating side, and retracted inside the blade on the advancing side.

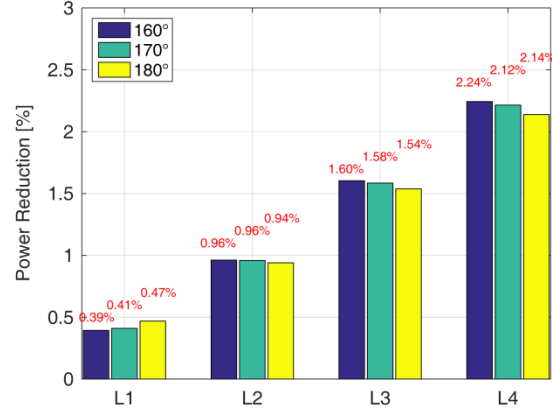


Figure 12: The effect of the location on the power reduction.

Figure 13 shows the power reduction with flight speed for different take-off weights. With the increase in the take-off weight, more power can be reduced, especially at high speed flight. At a speed of 280km/h, the take-off weight changes from 8322.3kg to 10627.0kg (weight coefficient from 0.0065 to 0.0083), and the power reduction increases from 0.43% to 2.33%. At larger take-off weight, the DEC can achieve power reduction over the whole speed range investigated. On the contrary, the DEC cannot reduce the rotor power with smaller take-off weight. Larger take-off weight or high thrust can upgrade the performance improvement by the DEC. By analogy, the DEC can achieve better performance at high flight altitude.

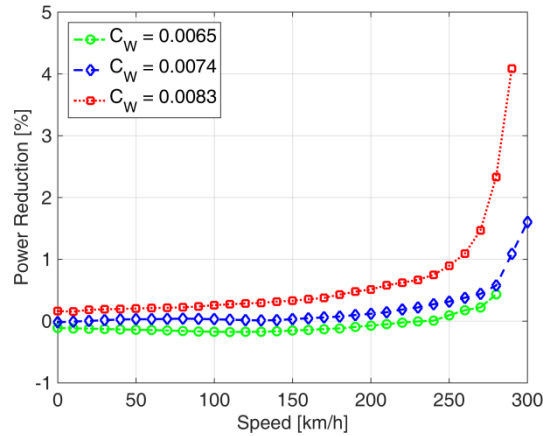


Figure 13: The effect of the weight on the power reduction.

Figure 14 compares the power reduction between a single DEC (Location 2 or Location 3) and two DEC (Location 2 with Location 3). For the DEC at Location 2 or Location 3, the phase is shifted to  $160^\circ$ . For the combined two DEC, the DEC at Location 3 shifts to  $160^\circ$ , and the phase of the DEC at Location 2 shifts to  $170^\circ$ . These are the optimum phases corresponding to maximum power reduction. The two DEC deliver more power reduction than a single DEC.

The power reduction of the two DEC is 2.40%, which is lower than the sum of 0.97% by the DEC at Location 2 and 1.60% at Location 3. So, interference between the two stations decreases the whole performance of the two DEC. The value of 2.40% is much larger than the value 1.90% by the STC with 20%c of chord extension at Location 2+3.

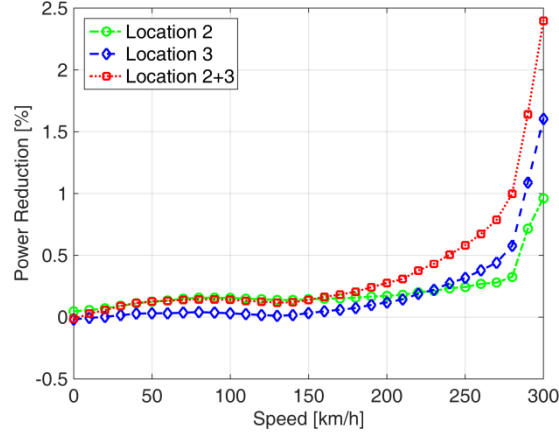


Figure 14 Two DEC for power reduction.

### 3.3 Dynamically Extendable Chord with Higher Harmonic Input

Figure 15 shows the power reduction for 2/rev input. From hover to medium forward speed flight, the power required increases. At high speed flight, the power reduction increases sharply if a suitable phase is used. The trend is similar as the 1/rev. The maximum power reduction is 1.21%, and this value is less than that obtained by the 1/rev. It indicates that the 1/rev DEC is more suitable for power reduction than the 2/rev. When the 2/rev DEC shifts to the optimum phase  $160^\circ$ , the power can be reduced when the speed is larger than 220km/h. No power saving could be obtained over the whole speed range investigated.

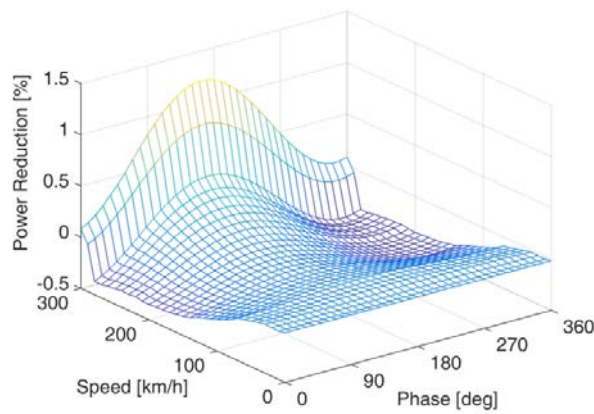


Figure 15 : Power reduction for the 2/rev input.

Figure 16 compares the power reductions by the SEC with different length and the DEC with different harmonic input at Location 3. For the DEC, the amplitude is 10%c and the phase is shifted to the optimum value corresponding to the maximum power reduction. The 1/rev input can obtain more power savings than the other harmonic inputs and SEC.

The 3/rev and 4/rev can reduce the rotor power at very high speed flight. Even at these speeds, the power reductions are small, and less than 1.0%. The SEC has similar performance as the higher harmonic input. SEC with larger lengths have more penalty in the power consumption than smaller ones from low to medium high speed flight. At very high speed flight, the larger chord is preferred. When using DEC for performance improvement of helicopters, one needs to consider carefully the corresponding penalties, such as actuation power consumption, structural weight, and system reliability.

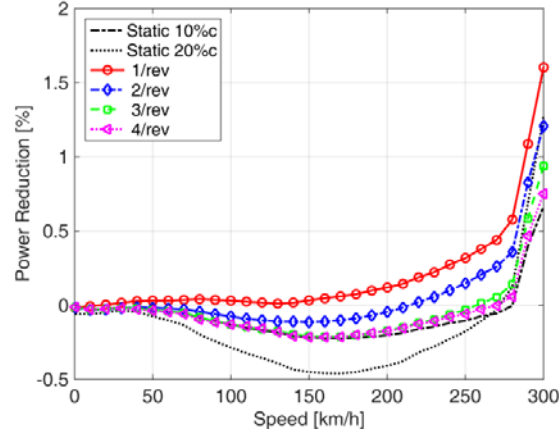


Figure 16: Power reduction for different strategies of the extendable chord.

#### 4. Conclusions

Statically and dynamically extendable chords (SEC/DEC) are assessed in rotor power reduction and helicopter performance improvement. A validated helicopter power estimation method is used to predict the rotor power with statically or dynamically extendable chords. It includes a rotor model, a fuselage model, a tail rotor model and a propulsive trim method. The analyses yielded the following conclusions:

1) In hover, the SEC can obtain rather small power savings when deployed in the mid-part of the blade. It also leads to an increase in the power at cruise. At high speed flight, it exhibits significant potential in power saving, and the best location for the power reduction is not the tip but inboard of it. **In the range of speed studied, the power reductions are less than 2.0%.**

2) The increase of the chord length of SEC can enhance power savings at high speed flight, but the performance at other speeds decreases.

3) The 1/rev DEC can obtain power reduction over the whole speed range, apart from hover and very low speed flight.

4) Unlike the SEC, the best deployment location of the 1/rev DEC is at the blade tip. It is best deployed on the retreating side and retracted back on the advancing side.

5) The increase in length of the chord extension and the helicopter take-off weight can enhance the power reduction by the 1/rev DEC. **At a takeoff weight coefficient of 0.0083 and forward speed of 280km/h, the rotor power can be reduced by 2.33%.**

6) Two 1/rev dynamic chords can obtain more power saving than an individual 1/rev chord, but the result is less than a single addition of the two savings.

7) The lower harmonic extendable chord can save more power than the higher harmonic excitation, and a dynamic chord reduces the power further than the static.

Finally, it is noted that the precise numbers given above are specific to the blade utilized in this work. For a rotor with

different planform, airfoils, diameter, etc., the optimum deployment and performance improvement levels may vary. The employed method can be easily used to assess the performance of other rotors with DEC/SEC.

### **Conflict of Interest Statement**

There is no conflict of interest

### **Acknowledgements**

This work was supported from the National Natural Science Foundation of China (11472129), and Science and Technology on Rotorcraft Aeromechanics Laboratory Foundation (6142220050416220002).

### **References**

- [1] Gessow, A., "Effect of Rotor-Blade Twist and Plan-form Taper on Helicopter Hovering Performance," NACA TN 1542, 1948.
- [2] Sikorsky, I. A., "Aerodynamic Parameters Selection in Helicopter Design," Journal of the American Helicopter Society, 1960, Vol. 5, No. 1, pp. 41-60.
- [3] McVeigh, M. A., and McHugh, F. J., "Influence of Tip Shape, Chord, Blade Number, and Airfoil on Advanced Rotor Performance," Journal of the American Helicopter Society, Vol. 29, No. 4, 1984, pp. 55-62.
- [4] Brocklehurst, A., and Barakos, G. N., "A Review of Helicopter Rotor Blade Tip Shapes," Progress in Aerospace Science, 2013, Vol. 56, pp. 35-74.
- [5] Walsh, J. L., Bingham, G. J., and Riley, M. F., "Optimization Methods Applied to the Aerodynamics Design of Helicopter Rotor Blades," Journal of the American Helicopter Society, Vol. 32, No. 4, 1987, pp. 39-44.
- [6] Leusink, D., Alfano, D., and Cinnella, P., "Multi-fidelity Optimization Strategy for the Industrial Aerodynamic Design of Helicopter Rotor Blades," Aerospace Science and Technology, 2015, Vol. 42, pp. 136-147.
- [7] Vu, N. A., and Lee, J. W., "Aerodynamic Design Optimization of Helicopter Rotor Blades including Airfoil Shape for Forward Flight," Aerospace Science and Technology, 2015, Vol. 42, pp. 106-117.
- [8] You, Y., Jung, S. N., "Optimum Active Twist Input Scenario for Performance Improvement and vibration of a helicopter rotor," Aerospace Science and Technology, 2017, Vol. 63, pp. 18-32.
- [9] Léon O., Hayden E., and Gandhi F., "Rotorcraft Operating Envelope Expansion using Extendable Chord Sections," the American Helicopter Society 65th Annual Forum, Grapevine, TX, USA, May 27-29, 2009, pp. 1940-1953.
- [10] Khoshlahjeh M., and Gandhi F., "Extendable Chord Rotors for Helicopter Envelope Expansion and Performance Improvement," Journal of the American Helicopter Society, 2014, Vol. 59, No. 1, pp. 0120071-01200710.
- [11] Kang H., Saberi H. and Gandhi F., "Dynamic Blade Shape for Improved Helicopter Rotor Performance," Journal of the American Helicopter Society, 2010, Vol. 59, No. 1, pp. 032008.
- [12] Peters, D. A. and HaQuang, N., "Dynamic Inflow for Practical Application," Journal of the American Helicopter Society, 1988, Vol.33, No.4, pp. 64-68.
- [13] Owen, D. R. J., and Hinton, E., "Finite Elements in Plasticity: Theory and Practice," Pineridge Press, Swansea, Wales, UK, 1980, pp. 431-436.
- [14] Han D., Wang H.-W., and Gao Z., "Aeroelastic Analysis of a Shipboard Helicopter Rotor with Ship Motions during Engagement and Disengagement Operations," Aerospace Science and Technology, 2012, Vol. 16, No. 1, pp. 1-9.
- [15] Han, D., Patrikakis, V. and Barakos, G., "Helicopter Performance Improvement by Variable Rotor Speed and Variable Blade Twist," Aerospace Science and Technology, 2016, Vol. 54, pp.164-173.
- [16] Yeo H., Bousman W.G., and Johnson W., "Performance Analysis of a Utility Helicopter with Standard and

Advanced Rotors,” Journal of the American Helicopter Society, 2004, Vol. 49, No. 3, pp. 250-270.

- [17] Hilbert, K. B., “A Mathematical Model of the UH-60 Helicopter,” Technical Report NASA-TM-85890, 1984.
- [18] Davis S. J., “Pre-design Study for a Modern 4-Bladed Rotor for the RSRA,” Technical Report NASA-CR-166155, 1981.
- [19] Bousman W. G., “Aerodynamic Characteristics of SC1095 and 1094R8 Airfoils,” Technical Report NASA/TP-2003-212265, 2003.
- [20] Bagai, A., “Aerodynamic Design of the X2 Technology Demonstrator<sup>TM</sup> Main Rotor Blade,” the American Helicopter Society 64th Annual Forum, Montreal, Canada, April 29-May 1, 2008.